Vailable online at www.sciencedirect.com

SciVerse ScienceDirect

Energy Procedia 27 (2012) 160 – 166

Energy Procedia

SiliconPV 2012, 03-05 April 2012, Leuven, Belgium

Characterization of oxidation-induced stacking fault rings in Cz silicon: Photoluminescence imaging and visual inspection after Wright etch

H. Angelskår[a*], R. Søndenå[a], M.S. Wiig[a], E.S. Marstein[a]

[a]*Institute for Energy Technology, Department for Solar Energy, P.O.Box 40, NO-2027 Kjeller, Norway*

Abstract

Oxidation-induced stacking fault rings in polished Cz silicon samples before and after thermal wet oxidation are investigated by use of photoluminescence imaging. Currently the standard procedure for OSF ring detection is to expose the samples to a toxic preferential etchant, e.g. a Wright solution, after a thermal oxidation. This solution primarily attacks the regions with stacking faults, allowing detection by visual inspection. Samples from the seed end of p-type Cz silicon ingots with resistivities of approximately 1 Ohm-cm were measured by PL imaging before and after a thermal oxidation process. Subsequently, Wright-etching was performed on the oxidized samples to expose stacking faults. The lifetime variations in the PL images were correlated with the location of the rings in the preferentially etched surfaces, and good agreement was found. The results show that for this crystal pulling process, even the PL images of unpassivated polished samples can be used to detect the OSF ring location. The thermal oxidation at 1100°C enhanced the contrast between the OSF ring and the rest of the sample in the PL image.

Keywords: Czochralski Silicon; oxidation-induced stacking faults; characterization; photoluminescence imaging; Wright etch

* Corresponding author. Tel.: +47 63806171; fax: +47 63812905
E-mail address: hallvard.angelskar@ife.no

1876-6102
doi:10.1016/j.egypro.2012.07.045

1. Introduction

Oxidation-induced stacking faults (OSFs) are occasionally observed in processed wafers from Cz silicon ingots where the oxygen concentration is high. The well-known OSF ring seen in horizontal cuts delineates a border between two regions: vacancy-type defects dominate on the inside of the ring, while the outside is dominated by silicon self-interstitials [1]. Before oxidation this border region can contain large grown-in oxygen precipitates forming the so-called P-band [2]. These oxygen precipitates can in turn act as nucleation sites for stacking faults during thermal oxidation, forming the OSF ring [3,4]. Recently, it has been shown that silicon wafers with oxygen-related defects have a significant negative impact on the efficiency of solar cells [5,6]. The OSF ring region is an important indicator of growth conditions and bulk properties, and can hence be used to optimize the useful part of the Cz silicon crystal. Detection of OSF rings is therefore of interest for both solar cell manufacturers and material producers.

Photoluminescence (PL) imaging [7] is a relatively new material and process characterization technique which has created a lot of interest in the photovoltaic community. The technique is very fast and sensitive, and is ideal for efficient characterization of bulk defects in relation to crystal growth. However, there are few reports related to PL imaging characterization of oxygen-related bulk defects in Cz ingots [5]. PL imaging yields a map of band-to-band luminescence intensity of the silicon sample. If the sample has homogeneous thickness and optical properties, the variations in PL intensity under steady state conditions (constant and homogeneous laser excitation) are due to variations in doping concentration and in injection level in the sample. If uniform doping can be assumed, the PL signal variations can be attributed to lifetime. The formation of an OSF ring is expected to change the recombination properties of the bulk, and should thus appear in the PL image, provided other defects do not dominate the lifetime.

In this work we investigate the detection of the OSF ring region by PL imaging of Cz silicon samples before and after a thermal oxidation process. The results of the PL imaging are compared with standard OSF detection processes, based on a visual inspection of the samples after a Wright etch which exposes the OSF rings.

2. Experimental

We report on measurements for two samples, A and B, from the seed end of two B-doped p-type Cz silicon ingots with 1 Ohm-cm resistivity, and oxygen concentration of approximately 19 ppm. The samples are semi-square with a diameter of 200 mm, and have a thickness of approximately 1.8 mm.
The surfaces are mechanically and chemically polished to avoid strong surface effects in the etching and PL imaging. Initial PL imaging of the polished samples is carried out before standard cleaning. Subsequently the samples were exposed to thermal wet oxidation at 1100°C for one hour. PL images of the oxidized samples are then acquired before oxide removal in a 5% HF solution is performed, after which a Wright etch is used to expose the OSF ring. The Wright solution is a pre-mixed solution from Gower Chemicals, composed of 10-20% acetic acid, 5-10% chromium trioxide, 10-20% hydrofluoric acid, 10-20% nitric acid. A comparison of PL images and optical images of the Wright etched samples is carried out. The lifetime of the samples was also mapped with microwave photoconductance decay (MW-PCD), in order to verify that the variations in the PL image were not due to doping density variations.

The PL images were measured with a LIS-R1 setup from BT Imaging, with an excitation laser of 808 nm wavelength and a cooled silicon CCD camera. All the PL images were acquired with 30 s exposure time. The thermal wet oxidation was carried out in a Tempress TS-8603 tube furnace. After the Wright etch, the photographs were taken whilst illuminating the samples with a collimated Xenon lamp. The light microscopy of the Wright-etched samples was carried out at 10x magnification.

3. Results and discussion

3.1. Photoluminescence imaging

The PL images for the seed end samples A and B show ring structure before oxidation (see Fig. 1 (a) and (b)). A dark band of low lifetime is seen, as indicated by white arrows from the center of the wafer to the center of the ring. This shows that the grown in microdefects and oxygen precipitates in the P-band have a detectable effect on the effective lifetime of unpassivated wafers, as reported previously in e.g. [8]. However, at this stage the ring structure could also be due to thermal donors, as discussed in [5]. A high-temperature anneal to kill thermal donors could be used to eliminate this possibility. However, it is shown below that the ring regions in Fig. 1 indeed correspond to the OSF ring region after oxidation.

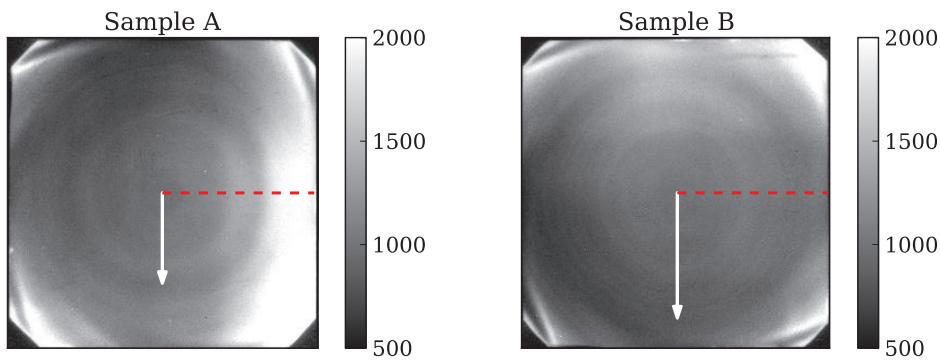

Fig. 1. Photoluminescence intensity images of the seed end samples before the oxidation process for Sample A (a) and Sample B (b)

After oxidation, in Fig. 2 (a) and (b), broader rings of relatively high lifetime (or PL signal) are seen. In the case of Sample B in Fig. 2 (b), the OSF ring overlaps with a high-lifetime region around the edge of the sample, known from the literature [3]. In Fig. 3 (a) and (b) we compare a linescan from the PL images before and after oxidation of sample A and B respectively. For sample A, the OSF ring is located approximately 50 mm from the center, and a slight dip in PL intensity before oxidation and a broad peak after oxidation is seen. The OSF ring region before oxidation is less clear for sample B due to low contrast in the image, but can be found at approximately 70 mm from the center. For both samples the PL image contrast could be improved by surface passivation. Samples from the tail end of the crystals were also measured and given the same thermal oxidation treatment, but as expected no ring patterns were seen.

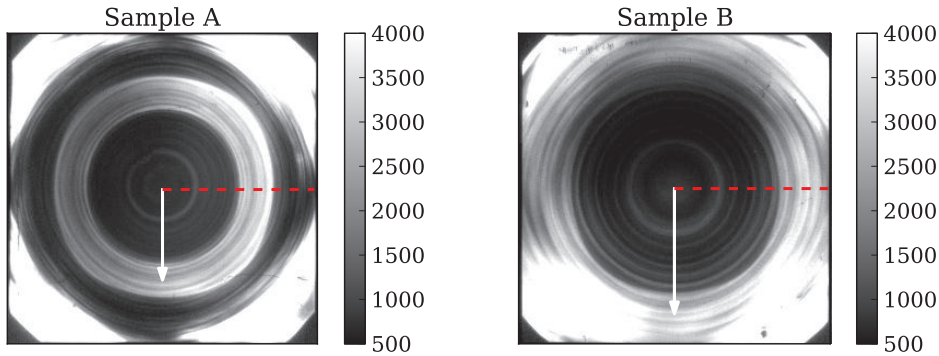

Fig. 2. Photoluminescence intensity images of the seed end samples after the oxidation process for Sample A (a) and Sample B (b). The oxide layer was not removed before the PL images were taken, however the same patterns are seen after oxide-removal and Wright etch

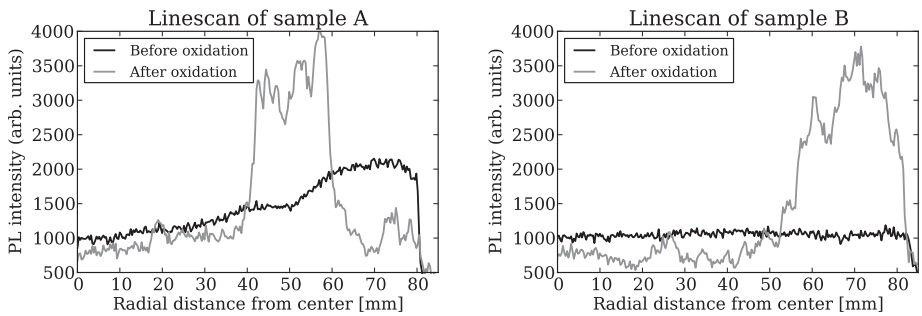

Fig. 3. (a) PL intensity line scans for Sample A along the red dashed lines in Fig. 1 (a) and Fig. 2 (a). The black curve corresponds to Fig. 1 a) before oxidation, and the gray curve to Fig. 2 a) after oxidation. The intensities before and after oxidation should not be directly compared, as the oxide layer was left on during the latter measurements; (b) PL intensity line scans for Sample B along the red dashed lines in Fig. 1 (b) and Fig. 2 (b)

3.2. Visual detection of OSFs after Wright etch

Fig. 4 (a) and (b) shows photographs of the Wright etched surfaces of sample A and B respectively illuminated by a collimated Xenon lamp. At this angle a bright light-scattering ring region is clearly seen. The microscope images from sample A in Fig. 5 (a) and (b) show that the density of etch pits is larger within the OSF ring (marked R in Fig. 4 (a)) compared to the middle of the sample (marked M in Fig. 4 (a)). The positions of the visually detected rings correspond to those marked by the arrows in the PL images, indicating that the low-lifetime ring regions in the PL images before oxidation (Fig. 1) are the nucleation sites of the stacking faults induced in the oxidation process.

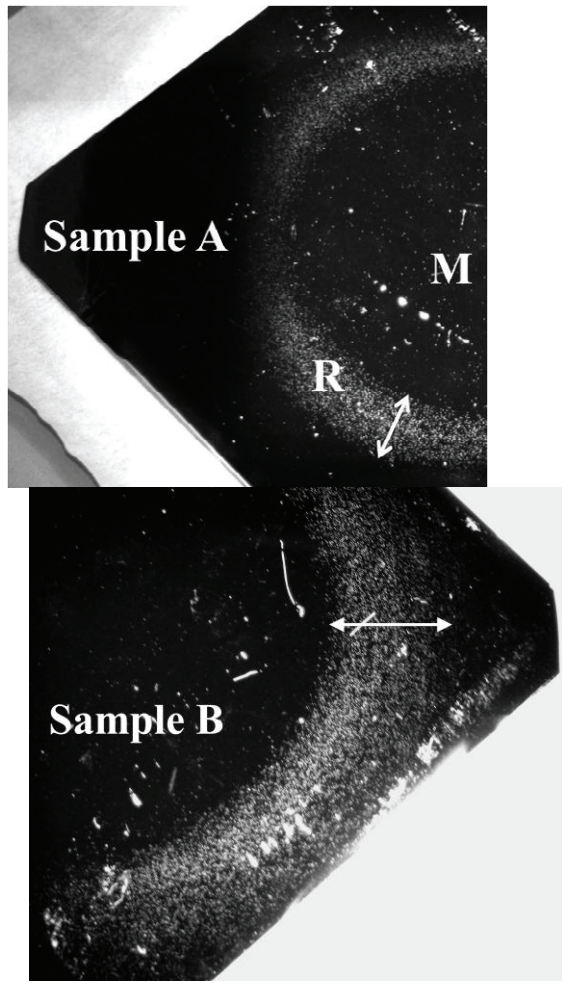

Fig. 4. (a) Photograph of sample A after Wright etch; (b) Photograph of sample B after Wright etch. The OSF rings are indicated by the white arrows

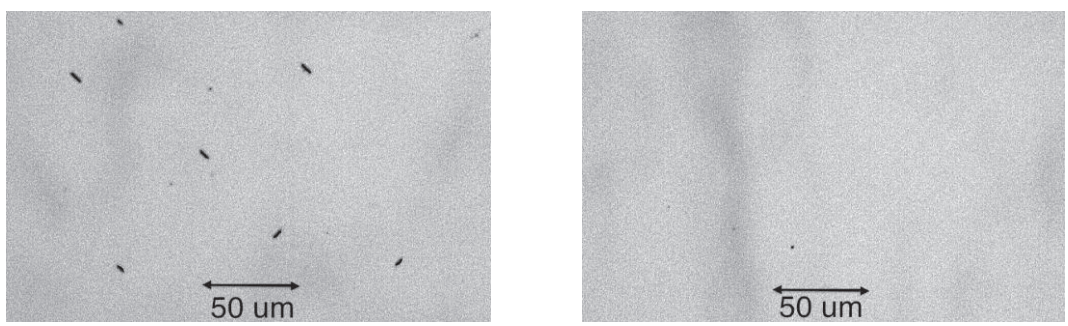

Fig. 5. (a) Microscope image from the ring region (marked R in Fig. 4 (a)); (b) Microscope image from the middle region inside the OSF ring (marked M in Fig. 4 (a))

3.3. Evolution of lifetime during thermal oxidation

The relatively high lifetime in the OSF ring region compared to the center region after oxidation (Fig. 2) is consistent with the literature: Depending on the thermal history of the crystal from the growth process, and on the temperature of the thermal oxidation, smaller oxygen precipitates inside and outside the P-band can grow during oxidation [2]. According to Porrini and Tessariol, the recombination activity of the oxygen precipitates increases strongly with the precipitate size [9]. Therefore, before oxidation, the recombination activity in the regions with a high density of smaller oxygen precipitates is lower than in the P-band. During oxidation the smaller oxide precipitates grow, resulting in an increased recombination activity which in turn may cause the reduced lifetime compared to the P-band or OSF region. Furthermore, it has been shown that in order for the stacking faults to form, the size of the oxygen precipitates need to be within certain limits [10]. A possible explanation for a low density of OSFs in the regions outside the OSF ring is then that the oxygen precipitates are too small for stacking faults to nucleate, while large and numerous enough to yield a significantly reduced lifetime.

4. Conclusion

OSF rings in p-type Cz silicon were studied with photoluminescence imaging and Wright etching. It was shown that for the present samples the P-band can be detected in PL images of polished unpassivated samples. After oxidation, the OSF ring region appears as a high-lifetime region relative to the rest of the sample, except for a high-lifetime region close to the crystals periphery. Before oxidation the P-band is seen in PL images as a low-lifetime ring region which correlates with the OSF ring as exposed by thermal wet oxidation and Wright etching. Thus, photoluminescence imaging can be used to optimize similar crystal growth processes, without the need for the toxic Wright etchant or the time and energy consuming thermal wet oxidation.

Acknowledgements

This work was performed within ”The Norwegian Research Centre for Solar Cell Technology” project number 193829, a Centre for Environment-friendly Energy Research co-sponsored by the Norwegian Research Council and research and industry partners in Norway. R. Falster is acknowledged for useful comments on OSFs.

References

[1] V. V. Voronkov, "The mechanism of swirl defect s formation in silicon", J. Cryst. Growth 59, 625-643 (1982).

[2] V. V. Voronkov and R. Falster, “Grown-in microdefects, residual vacancies and oxygen precipitation bands in Czochralski silicon”, J. Cryst. Growth 204, 462-474 (1999).

[3] R. A. Brown, Z. Wang, and T. Mori, “Engineering analysis of microdefect formation during silicon crystal growth”, J. Cryst. Growth 225, 97-109 (2001).

[4] M. Hasebe, Y. Takeoka, S. Shinoyama, S. Naito, “Formation process of Sracking Faults with Ringlike Distribution in CZ-Si Wafers”, Jpn. J. Appl. Phys. 34, 1999-2002 (1989).

[5] J. Haunschild, I. E. Reis, J. Geilker and S. Rein, “Detecting efficiency-limiting defects in Czochralski-grown silicon wafers in solar cell production using photoluminescence imaging”, Phys. Status Solidi RRL 5, 199-201 (2011).

[6] P.J. Cousins, D. D. Smith, H. C. Luan, J. Manning, T. D. Dennis, A. Waldhauer, K. E. Wilson, G. Harley, W. P. Mulligan, “Generation 3: Improved performance at lower cost”, 35th IEEE PVSC, Hawaii, USA (2010).

[7] T. Trupke, R. A. Bardos, M. C. Schubert, and W. Warta, “Photoluminescence imaging of silicon wafers”, Appl. Phys. Lett. 89, 044107 (2006).

[8] N. Ikeda, A. Buczkowski, F. Shimura, “Noncontact characterization for grown-in defects in Czochralski silicon wafers with a laser/microwave photoconductance method”, Appl. Phys. Lett. 63, 2914-6 (1993).

[9] M. Porrini and P. Tessariol, “Minority carrier lifetime of p-type silicon containing oxygen precipitates: influence of injection level and precipitate size/density”, Mat. Sci. Eng., B 73, 244-9 (2000).

[10] K. Marsden, S. Sadamitsu, T. Yamamoto, T. Shigematsu, “Generation of Oxidation-Induced Stacking Faults in Czochralski-Grown Silicon Crystals Exhibiting a Ring-like Distributed Stacking Fault Region”, Jpn. J. Appl. Phys. 34, 2974-2980 (1995).